

Realistic description of electron-energy loss spectroscopy for one-Dimensional Sr_2CuO_3

A. Hübsch,^a J. Richter,^a C. Waidacher,^a K. W. Becker,^a and W. von der Linden^b

(a) *Institut für Theoretische Physik, Technische Universität Dresden, D-01062 Dresden, Germany*

(b) *Institut für Theoretische Physik, Technische Universität Graz, Petersgasse 16, A-8010 Graz, Austria*

We investigate the electron-energy loss spectrum of one-dimensional undoped CuO_3 chains within an extended multi-band Hubbard model and an extended one-band Hubbard model, using the standard Lanczos algorithm. Short-range intersite Coulomb interactions are explicitly included in these models, and long-range interactions are treated in random-phase approximation. The results for the multi-band model with standard parameter values agree very well with experimental spectra of Sr_2CuO_3 . In particular, the width of the main structure is correctly reproduced for all values of momentum transfer. We find no evidence for enhanced intersite interactions in Sr_2CuO_3 .

PACS numbers: 71.27.+a, 71.45.Gm, 71.10.Fd

One-dimensional systems are easy to conceive in theory but hard to find in nature, and their experimental realization is restricted to few materials. These include mesoscopic systems like single-wall nanotubes^{1,2} or chains of metal atoms,³⁻⁵ and macroscopic systems with a strong anisotropy in one spatial direction. Among the latter, Sr_2CuO_3 has been in the focus of recent research. It contains separated chains of corner-sharing CuO_4 plaquettes, and is related to high-temperature superconducting compounds of higher dimensionality. Generally, the electronic properties of Sr_2CuO_3 are dominated by strong correlations of the valence holes. The low-dimensional character of magnetic excitations in this material manifests itself in magnetic susceptibility measurements that have been successfully described in terms of a one-dimensional spin- $\frac{1}{2}$ Heisenberg antiferromagnet.⁶⁻⁸

Charge excitations in Sr_2CuO_3 have recently been investigated⁹ by means of electron energy-loss spectroscopy (EELS). The experimental spectra are shown in the right panel of Fig. 1. In the following we will only discuss the spectral region below 4eV energy loss. Excitations at higher energies probably involve Sr orbitals, which are not included in models for the Cu-O structure.⁹ In the low energy region the experimental data show a broad dominant low-energy structure at 2.4 eV for momentum transfer $\mathbf{q} = 0.1\text{\AA}^{-1}$, which shifts to 3.2eV for $\mathbf{q} = 0.8\text{\AA}^{-1}$ [see Fig. 1]. The behavior of this structure as a function of momentum transfer is rather unusual: with increasing momentum transfer up to 0.4\AA^{-1} the width of the structure decreases but increases again for $\mathbf{q} > 0.4\text{\AA}^{-1}$. These spectra have been interpreted using an extended one-band Hubbard model,⁹ an effective two-band Hubbard model,¹⁰ and a multi-band Hubbard model.¹¹ Although the main difference between these models is just the elimination of the oxygen degrees of freedom, the results have been discussed controversially. In the one-band model the behavior of the low-energy feature has been interpreted as the transfer of spectral weight from a continuum of excitations to an exciton, formed due to a strongly enhanced intersite Coulomb repulsion V .^{9,12} Excitonic features have also been discussed in the strong coupling limit of an effective two-band Hub-

bard model.¹⁰ However, the used coupling strengths are not experimentally relevant. Therefore, no direct comparison to experimental data was possible in Ref. 10. In contrast, in the multi-band model the dispersion of the low-energy feature has been explained in terms of a shift from a rather delocalized Zhang-Rice singlet-like excitation to a more localized one.¹¹ However, no intersite Coulomb repulsion was included in the Hamiltonian.

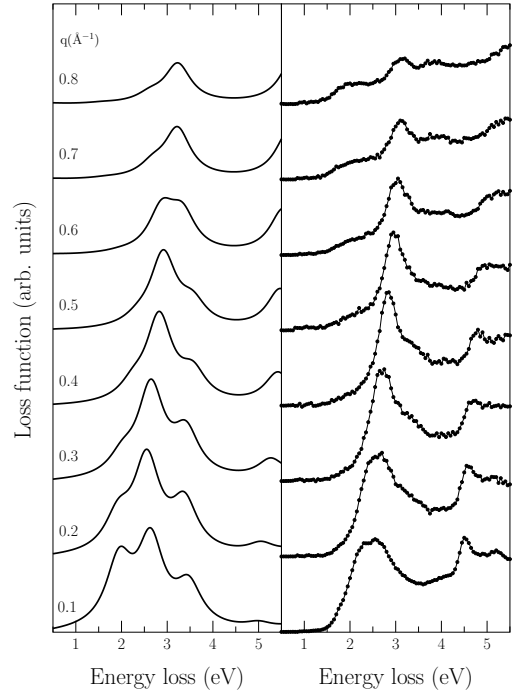


FIG. 1. Comparison of experimental data for Sr_2CuO_3 (right panel), taken from Ref. 9, and the results of the exact diagonalization (left panel). The parameter set is $U_d = 8.8\text{eV}$, $\Delta = 3.0\text{eV}$, $V_{pd} = 1.2\text{eV}$, $V_{dd} = 0\text{eV}$, $t_{pd} = 1.3\text{eV}$, and $t_{pp} = 0.65\text{eV}$. The theoretical line spectra have been convoluted with a Gaussian function of width 0.35eV .

Up to now, all theoretical approaches failed to correctly describe the discussed decrease and increase in spectral width of the low-energy feature as a function

of increasing momentum transfer: For small momentum transfer, the one-band model overestimates the experimentally observed width by a factor of about two.⁹ In addition, the broadening for large momentum transfer is too small. The analytical approach to the multi-band model, on the other hand, underestimates the broadening due to the neglect of far reaching excitations that are important at small momentum transfer.¹¹

In this paper, we show that the multi-band model provides a realistic description of the EELS spectrum for Sr₂CuO₃, and we observe the correct spectral form for all values of momentum transfer. Furthermore, it is found that the main effect of the intersite Coulomb repulsion is to lead to an energy shift of the EELS spectra. Finally, we discuss the relations of our results to the loss function of the one-band model.

We investigate the dielectric response of a one-dimensional extended multi-band Hubbard Hamiltonian at half-filling, i.e. a chain of corner-sharing CuO₄ plaquettes with one hole per Cu site. In the hole picture this Hamiltonian reads^{13,14}

$$\begin{aligned}
H = & \Delta \sum_{j\sigma} n_{j\sigma}^p + U_d \sum_i n_{i\uparrow}^d n_{i\downarrow}^d \\
& + V_{pd} \sum_{\langle ij \rangle} n_j^p n_i^d + V_{dd} \sum_{\langle ii' \rangle} n_i^d n_{i'}^d \\
& + t_{pd} \sum_{\langle ij \rangle \sigma} \phi_{pd}^{ij} (p_{j\sigma}^\dagger d_{i\sigma} + \text{H.c.}) \\
& + t_{pp} \sum_{\langle jj' \rangle \sigma} \phi_{pp}^{jj'} p_{j\sigma}^\dagger p_{j'\sigma} .
\end{aligned} \quad (1)$$

The operators $d_{i\sigma}^\dagger$ ($p_{j\sigma}^\dagger$) create a hole with spin σ in the i -th Cu $3d$ orbital (j -th O $2p$ orbital), and $n_{i\sigma}^d$ ($n_{j\sigma}^p$) are the corresponding number operators, with $n_i^d = n_{i\uparrow}^d + n_{i\downarrow}^d$. The first four terms in Eq. (1) are the atomic part of the Hamiltonian, with the charge-transfer energy Δ , the Cu on-site Coulomb repulsion U_d , the Cu-O intersite repulsion V_{pd} , and the Cu-Cu intersite repulsion V_{dd} . The last two terms in Eq. (1) describe the hybridization of Cu $3d$ and O $2p$ orbitals (hopping strength t_{pd}) and of O $2p$ orbitals (hopping amplitude t_{pp}). ϕ_{pd}^{ij} and $\phi_{pp}^{jj'}$ give the correct sign for the hopping processes, and $\langle ij \rangle$ denotes the summation over nearest neighbor pairs. Hamiltonian (1) takes account of both in-chain and out of chain oxygen sites. Notice that no perturbative approximations are made, so that parameter values can be chosen in the experimentally relevant range.

The dynamical density-density correlation function is directly proportional to the loss function in EELS experiments.¹⁵ By including the long-range Coulomb interaction in the model within a random-phase approximation¹⁶ (RPA) one finds for the loss function

$$L(\omega, \mathbf{q}) = \text{Im} \left[\frac{-1}{1 + v_{\mathbf{q}} \chi_{\rho}^0(\omega, \mathbf{q})} \right], \quad (2)$$

where

$$\chi_{\rho}^0(\omega, \mathbf{q}) = \frac{i}{\hbar} \int_0^{\infty} dt e^{i\omega t} \langle 0 | [\rho_{\mathbf{q}}(t), \rho_{-\mathbf{q}}] | 0 \rangle \quad (3)$$

is the response function at zero temperature of the short-range interaction model (1). χ_{ρ}^0 depends on the energy loss ω and momentum transfer \mathbf{q} . $|0\rangle$ is the ground state, $\rho_{\mathbf{q}}$ denotes the Fourier transform of n_i , and $v_{\mathbf{q}} = e^2 N / (\epsilon_0 \epsilon_r v \mathbf{q}^2)$ is the long-range Coulomb interaction with unit cell volume v . N is the number of electrons per unit cell, and ϵ_o is the permittivity. The real part ϵ_r of the dielectric function can be obtained from the experiment. In the case of Sr₂CuO₃ it was found to be $\epsilon_r = 8$.⁹ In the following we evaluate Eq. (2) using the standard Lanczos algorithm¹⁷ which is limited to small clusters. The theoretical line spectra are convoluted with a Gaussian function of width 0.35eV, to allow a comparison with the experiment.

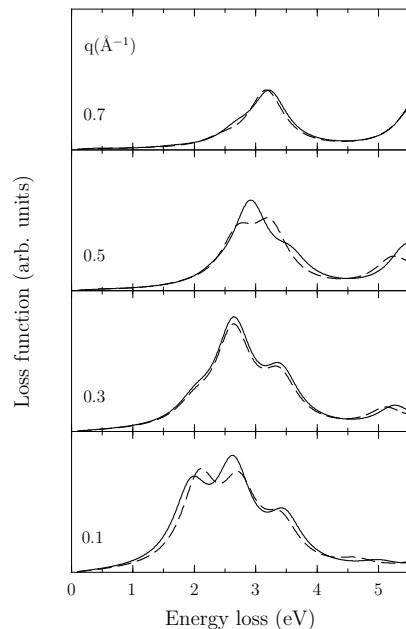


FIG. 2. Finite-size effects in the loss function of model (1) for clusters with six plaquettes (full lines) and five plaquettes (dashed line), with open boundary conditions. Parameters as for Fig. 1.

First we check if our results are sufficiently converged with respect to system size. In Fig. 2 we compare the loss function of clusters with five (dashed lines) and six plaquettes (full lines). In both cases open boundary conditions are chosen. One has to make sure that holes on the edges of the cluster are still embedded in the local Coulomb potential that results from a state with occupied Cu sites. For this purpose, O (Cu) sites on the edge of the cluster are assigned an additional on-site energy due to V_{pd} (V_{dd}). As can be seen from Fig. 2, there are only small finite-size effects. Thus we conclude that the cluster with six plaquettes is large enough to obtain reliable results.

In Fig. 1 the calculated loss function is compared to the experimental spectra from Ref. 9. The parameters in the model Hamiltonian are chosen as follows: $U_d = 8.8\text{eV}$, $V_{pd} = 1.2\text{eV}$, $V_{dd} = 0\text{eV}$, $t_{pd} = 1.3\text{eV}$ and $t_{pp} = 0.65\text{eV}$ are kept constant at typical values.^{18–20} The value of $\Delta = 3.0\text{eV}$ has been adjusted to obtain correct peak positions. This means that we use only one free parameter. As compared to the standard value 3.5eV for Δ ,^{18–20} the smaller Δ is in agreement with theoretical analysis of x-ray photoemission spectra for Sr_2CuO_3 .^{25,22,23} Notice that a small value of Δ means that the system is not in the strong coupling limit as was assumed in Ref. 10. The calculated loss function consists of a dominant structure at 2.5eV for $\mathbf{q} = 0.1\text{\AA}^{-1}$, which shifts to 3.2eV for $\mathbf{q} = 0.8\text{\AA}^{-1}$. Besides, a second excitation is observed at 5.5eV . In agreement with the experimental observation, with increasing momentum transfer the main structure shifts to higher energies and first decreases in width. For $\mathbf{q} > 0.4\text{\AA}^{-1}$ the spectral width increases again. The main structure results from excitations in which a hole leaves its original plaquette to form Zhang-Rice singlet-like states²⁴ with neighboring holes. With increasing momentum transfer \mathbf{q} the spectral weight shifts from extended to more localized excitations.¹¹

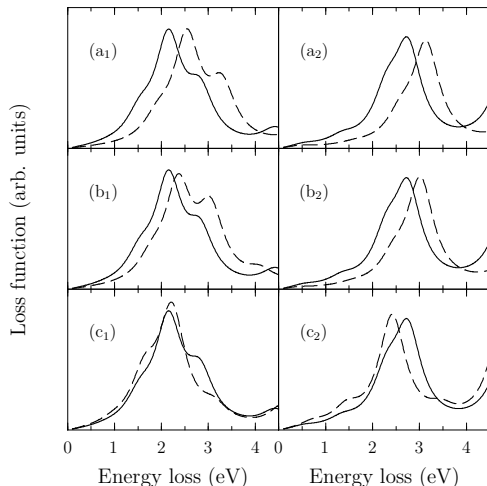


FIG. 3. Influence of V_{pd} , Δ , and V_{dd} on the loss functions with momentum transfer $\mathbf{q} = 0.3\text{\AA}^{-1}$ (left side) and $\mathbf{q} = 0.7\text{\AA}^{-1}$ (right side); other parameters as for Fig. 1. In (a) $\Delta = 3.0\text{eV}$ and V_{dd} are kept constant and V_{pd} is varied (full line: $V_{pd} = 0$, dashed line: $V_{pd} = 1.0\text{eV}$), in (b) Δ is varied (full line: $\Delta = 3.0\text{eV}$, dashed line: $\Delta = 4.0\text{eV}$) for $V_{pd} = V_{dd} = 0$, and in (c) $\Delta = 3.0\text{eV}$ and $V_{pd} = 0$ are constant (full line: $V_{dd} = 0$, dashed line: $V_{dd} = 0.5\text{eV}$). The loss functions with $\mathbf{q} = 0.3\text{\AA}^{-1}$ and $\mathbf{q} = 0.7\text{\AA}^{-1}$ are scaled independently of each other.

Next we discuss the dependence of the calculated spectra on the different parameters in Hamiltonian (1). In agreement with an analysis²⁵ of the optical conductivity for Sr_2CuO_3 it is found that the main influence of Δ and the intersite Coulomb repulsion V_{pd} is a shift of the excitation energy of the main structure. This is shown

in Fig. 3 for V_{pd} [see panels (a₁) and (a₂)] and Δ [see panels (b₁) and (b₂)]. Note that we observe nearly the same results for $\Delta = 3.0\text{eV}$, $V_{pd} = 1.0\text{eV}$ [dashed lines in panels (a₁) and (a₂) of Fig. 3] and $\Delta = 4.0\text{eV}$, $V_{pd} = 0$ [dashed lines in panels (b₁) and (b₂) of Fig. 3]. Hence, only the sum of both parameters $\Delta + V_{pd}$ is relevant for the spectra. Therefore, it is possible to obtain good agreement between experimental and theoretical spectra with or without intersite Coulomb interaction V_{pd} . This implies that the mechanism of excitations is not driven by a strong intersite interaction V_{pd} . Furthermore, this observation also explains why a fit of a multi-band model with $V_{pd} = 0$ to the experimental data has led to a larger value of Δ in Ref. 11.

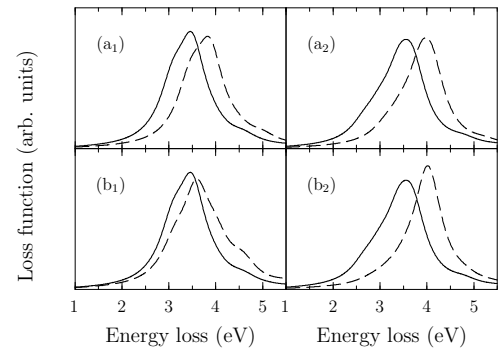


FIG. 4. Influence of the Coulomb interactions U and V of the extended one-band Hubbard model on the loss function with momentum transfer $\mathbf{q} = 0.3\text{\AA}^{-1}$ (left side) and $\mathbf{q} = 0.7\text{\AA}^{-1}$ (right side); parameter values are chosen according to Ref. 9. The hopping strength is $t = 0.55\text{eV}$. In (a) $V = 1.3\text{eV}$ is kept constant (full line: $U = 4.2\text{eV}$, dashed line: $U = 4.7\text{eV}$), and in (b) V is varied (full line: $V = 1.3\text{eV}$, dashed line: $V = 0.8\text{eV}$) for $U = 4.2\text{eV}$. The theoretical line spectra have been convoluted with a Gaussian function of width 0.35eV . The loss functions with $\mathbf{q} = 0.3\text{\AA}^{-1}$ and $\mathbf{q} = 0.7\text{\AA}^{-1}$ are scaled independently of each other.

In contrast to Δ and V_{pd} , the Cu-Cu intersite repulsion V_{dd} does not shift the complete EELS spectra but rather transfers spectral weight to excitations with smaller energy loss [see panels (c₁) and (c₂) of Fig. 3]. A comparison of panels (c₁) and (c₂) shows that this effect is larger near the zone boundary at $\mathbf{q} = 0.8\text{\AA}^{-1}$. Probably, this behavior can be connected with a formation of an exciton state as discussed in Ref. 9,10. On the other hand, the choice $V_{dd} = 0$ is a good approximation²⁶ for the multi-band model (1) since the distance between neighboring Cu sites is relatively large. Therefore, a possible exciton formation seems not to be relevant for the interpretation of the experimental spectra if one uses the multi-band model.

Finally, we want to discuss the relation of our results for the multi-band model to the loss function (2) of the one-dimensional extended Hubbard model

$$H = -t \sum_{\langle ij \rangle \sigma} (d_{i\sigma}^\dagger d_{j\sigma} + \text{H.c.}) + U \sum_i n_{i\uparrow}^d n_{i\downarrow}^d + V \sum_{\langle ij \rangle} n_i^d n_j^d \quad (4)$$

which only considers effective Cu 3d orbitals. In Eq. (4), t is the hopping strength, U denotes the on-site Coulomb repulsion, and V is the intersite interaction. Note that the mapping of the multi-band model (1) onto the one-band model (4) is problematic for the model parameters used above because the system is not in the strong coupling limit. Therefore, we may compare the loss function of both models only qualitatively. In the following, we compute the loss function (2) of the one-band model (4) using a cluster with twelve sites and periodic boundary conditions. If one reduces the multi-band model (1) to a one-band model the charge-transfer gap Δ is replaced by the Hubbard gap U of the effective model.²⁷ Therefore, in analogy to the influence of Δ in the multi-band model, increasing U shifts the spectra to higher energy loss [see panels (a₁) and (a₂) of Fig. 4]. In panels (b₁) and (b₂) of Fig. 4 the loss functions with $\mathbf{q} = 0.3\text{\AA}^{-1}$ and $\mathbf{q} = 0.7\text{\AA}^{-1}$ are shown for $V = 1.3\text{eV}$ (full lines) and $V = 0.8\text{eV}$ (dashed lines) where $U = 4.2\text{eV}$ and $t = 0.55\text{eV}$ are kept constant at the values from Ref. 9. In analogy to the influence of the intersite Coulomb repulsion V_{dd} in the multi-band model discussed above, a moderate increase in V leads mainly to a transfer of spectral weight to excitations with smaller energy loss. However, a non-zero intersite Coulomb repulsion V is needed to obtain spectra related to the experiment. This fact led to the conclusion that the spectral intensity at the zone boundary is due to an exciton formation.⁹ On the other hand, the large differences between the interpretations of the experimental spectra for Sr₂CuO₃ using the one-band⁹ and the multi-band model imply that oxygen degrees of freedom are important for a realistic description of charge excitations in the cuprates.

In conclusion, we have carried out an investigation of the EELS spectrum for the one-dimensional CuO₃ chain using an extended multi-band Hubbard model and an extended Hubbard model. Our results for the multi-band model show very good agreement with experimental data for Sr₂CuO₃. In contrast to former investigations, we can explain the width of the main structure for all values of momentum transfer. For the multi-band model, only a combination of intersite Coulomb interaction and charge-transfer energy is relevant for the loss function. Consequently, we find no evidence for enhanced intersite interactions in Sr₂CuO₃. The different explanations for the spectral intensity at the zone boundary using the one-band and the more realistic multi-band model shows that the oxygen degrees of freedom are important for the description of charge excitations.

We would like to acknowledge fruitful discussions with S. Atzkern, S.-L. Drechsler, J. Fink, M. S. Golden, R. E. Hetzel, R. Neudert, and H. Rosner. This work was supported by DFG through the research programs GK 85

and SFB 463. The calculations were performed on the Origin 2000 at Technische Universität Dresden.

-
- ¹ S. Ijima, *Nature* **345**, 56 (1991).
 - ² M. Bockrath, D. H. Cobden, J. Lu, A. G. Rinzler, R. E. Smalley, L. Balents, and P. L. McEuen, *Nature* **397**, 598 (1999).
 - ³ H. Brune, M. Giovannini, K. Bromann, and K. Kern, *Nature* **394**, 451 (1998).
 - ⁴ A. I. Yanson, G. Rubio Bollinger, H. E. van den Brom, N. Agrat, and M. van Ruitenbeek, *Nature* **395**, 783 (1998).
 - ⁵ P. Segovia, D. Purdie, M. Hengsberger, and Y. Baer, *Nature* **402**, 504 (1999).
 - ⁶ T. Ami, M. K. Crawford, R. L. Harlow, Z. R. Wang, D. C. Johnston, Q. Huang, and R. W. Erwin, *Phys. Rev. B* **51**, 5994 (1995).
 - ⁷ N. Motoyama, H. Eisaki, and S. Uchida, *Phys. Rev. Lett.* **76**, 3212 (1996).
 - ⁸ K. M. Kojima, Y. Fudamoto, M. Larkin, G. M. Luke, J. Merrin, B. Nachumi, Y. J. Uemura, N. Motoyama, H. Eisaki, S. Uchida, K. Yamada, Y. Endoh, S. Hosoya, B. J. Sternlieb, and G. Shirane, *Phys. Rev. Lett.* **78**, 1787 (1997).
 - ⁹ R. Neudert, M. Knupfer, M. S. Golden, J. Fink, W. Stephan, K. Penc, N. Motoyama, H. Eisaki, and S. Uchida, *Phys. Rev. Lett.* **81**, 657 (1998).
 - ¹⁰ K. Penc and W. Stephan, *Phys. Rev. B* **62**, 12707 (2000).
 - ¹¹ J. Richter, C. Waidacher, and K. W. Becker, *Phys. Rev. B* **61**, 9871 (2000).
 - ¹² W. Stephan and K. Penc, *Phys. Rev. B* **54**, R17269 (1996).
 - ¹³ V. J. Emery, *Phys. Rev. Lett.* **58**, 2794 (1987).
 - ¹⁴ V. J. Emery and G. Reiter, *Phys. Rev. B* **38**, 4547 (1988).
 - ¹⁵ S. E. Schnatterly, *Solid State Phys.* **34**, 275 (1977).
 - ¹⁶ D. Pines and D. Bohm, *Phys. Rev.* **85**, 338 (1952).
 - ¹⁷ For example, see H. Q. Lin and J. E. Gubernatis, *Computer in Physics* **7**, 400 (1993), and references therein.
 - ¹⁸ A. K. Mahan, R. M. Martin, and S. Satpathy, *Phys. Rev. B* **38**, 6650 (1988).
 - ¹⁹ M. S. Hybertsen, M. Schlüter, and N. E. Christiansen, *Phys. Rev. B* **39**, 9028 (1989).
 - ²⁰ J. B. Grant and A. K. McMahan, *Phys. Rev. B* **46**, 8440 (1992).
 - ²¹ K. Okada, A. Kotani, K. Maiti, and D. D. Sarma, *J. Phys. Soc. Jpn.* **65**, 1844 (1996).
 - ²² C. Waidacher, J. Richter, and K. W. Becker, *Europhys. Lett.* **47**, 77 (1999).
 - ²³ C. Waidacher, J. Richter, and K. W. Becker, *Phys. Rev. B* **61**, 13473 (2000).
 - ²⁴ F. C. Zhang and T. M. Rice, *Phys. Rev. B* **37**, 3759 (1988).
 - ²⁵ K. Okada and A. Kotani, *J. Phys. Soc. Jpn.* **66**, 341 (1997).
 - ²⁶ E. Dagotto, *Rev. Mod. Phys.* **66**, 763 (1994).
 - ²⁷ J. Zaanen, G. A. Sawatzky, and J. W. Allen, *Phys. Rev. Lett.* **55**, 418 (1985).